LETTERS SCIENCE CHINA Materials

mater.scichina.com link.springer.com

Published online 16 March 2015 | doi: 10.1007/s40843-015-0035-4
Sci China Mater 2015, 58: 186–191

Green light-emitting diode from bromine based organic-inorganic halide perovskite

Xiang Qin[1,2], Huanli Dong[1*] and Wenping Hu[1*]

Organic-inorganic halide perovskites have attracted considerable attention owing to their outstanding solar cell efficiency. Meanwhile, these halide perovskites exhibit good light emitting in visible and near-infrared range with high fluorescence quantum yield, resulting in electroluminescence. However, it remains challenging for lighting and display due to the low luminance and poor long-term stability. Herein, high performance green light-emitting diodes are fabricated from bromine based perovskite ($CH_3NH_3PbBr_3$) by systematically adjusting the preparation conditions and optimizing the emitting layer thickness. A high luminance up to 1500 cd m^{-2} (one of the highest values for perovskites-based light-emitting diodes) was achieved with 80 nm perovskites-emitting layer, due to the well-crystallized, full-coverage property of the films. This result further confirms the great prospect of organic-inorganic perovskites in optoelectronics.

Recently, organic-inorganic halide perovskites, a new class of semiconductors with high power conversion efficiency and long-range balanced hole-electron transport characteristics, have shown huge potential in photovoltaics [1–10]. However, the work principle of these perovskite materials has not been well elucidated except for a few reports [11–15]. Apart from charge mobility [16,17], optical properties clearly point out another way to investigate these materials, which show pieces of information including charge separation, bandgap and chemical purity [18]. Interestingly, these organic-inorganic materials based on perovskites really exhibit excellent photoluminescence properties with tunable visible and near-infrared spectrum [19–22]. Moreover, combined with their balanced ambipolar properties, these materials have been proven to be electrically light emission. Very recently, a breakthrough in light-emitting diodes (LEDs) based on organic-inorganic halide perovskites has been made, which proves organic-inorganic halide perovskites as promising candidates in LEDs [23]. The ever reported LEDs based on these halide perovskites which show electroluminescence in near-infrared, red and green region and a luminance of ~364 cd m^{-2} was achieved when the thickness of the active layer was 20 nm. Lately, an improved luminance of 417 cd m^{-2} was obtained for multicolored perovskites-LEDs based on a 40 nm emitter layer, which is due to the reduced carrier injection barrier for efficient electroluminescence [24]. However, further application remains challenging owing to the toxicity of Pb atom, poor long-term stability and low luminance. Thus, improving the luminance, which is the focus of this paper, emerges as an important and urgent aspect to make these LEDs commercialized.

According to previous reports, the efficiency of organic-inorganic halide perovskites based LEDs strongly depends on the quality of the emitting layer, such as thickness, crystallinity and coverage. Herein, we successfully fabricated a bromine based perovskite LED by a vapor method under atmosphere and evaluated the characteristics of the prepared perovskite LED at room temperature. In the device, $CH_3NH_3PbBr_3$ was chosen as the emitting layer, which was more stable than $CH_3NH_3PbI_3$ [25]. Attractively, high quality of emitter was achieved with well-crystallized, full-coverage and optimized thickness. Thanks to the high-quality emitting layer, the device showed brightly green emission with high color purity and exhibited high luminance at 1000 cd m^{-2}, with the highest luminance up to 1500 cd m^{-2}. However, there was no significant optimization in external quantum efficiency (EQE) compared with the previously reported LEDs.

In the green LED, a simple structure of indiumtin oxide (ITO)/poly(3,4-ethylenedioxythiophene): poly(styrenesulfonate) (PEDOT:PSS) (30 nm)/$CH_3NH_3PbBr_3$/1,3,5-tri[(3-pyridyl)-phen-3-yl]benzene(TmPyPB)(60 nm)/LiF(2 nm)/Al(100 nm) was fabricated as shown in Fig. 1. In this structure, ITO and Al are the anode and cathode, respectively, while LiF serves as the cathode buff layer. PEDOT:PSS and TmPyPB separately takes the role of hole-transport and electron-transport layers. The critical layer for green emission is the perovskite layer. The fabrication of the green perovskite LED was carried out under ambient condition.

[1] Beijing National Laboratory for Molecular Sciences, Key Laboratory of Organic Solids, Institute of Chemistry, Chinese Academy of Sciences, Beijing 100190, China
[2] University of Chinese Academy of Sciences, Beijing 100190, China
[*] Corresponding authors (emails: dhl522@iccas.ac.cn (Dong H); huwp@iccas.ac.cn (Hu W))

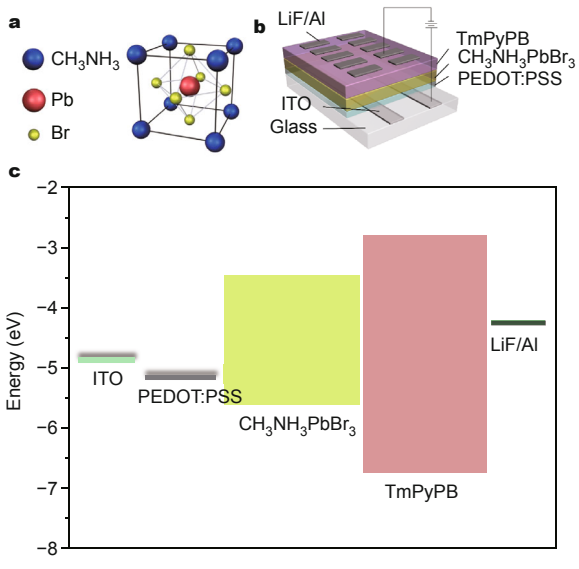

Figure 1 Structure and energy level of the bromine based perovskite LED. (a) Single unit cell of a $CH_3NH_3PbBr_3$ crystal; (b) device structure of the perovskite LED; (c) energy level of different layers.

Firstly, PEDOT:PSS was spin-coated onto the patterned ITO substrate at 3000 rpm for 30 s and then annealed at 120°C for 20 min. A planar $CH_3NH_3PbBr_3$ emitter layer was represented via a vapor-assisted solution process [26]. Then, the TmPyPB layer was deposited at a rate of 2 A s^{-1} with a base pressure at 10^{-6} Torr. Finally, the typical deposition rates of 0.1 A s^{-1} for LiF buffer layer and 0.6 A s^{-1} for Al layer at 10^{-6} Torr were carried out to complete the device.

It is well-known that the quality of the perovskite layer affects the performance of the device greatly. To prepare the critical $CH_3NH_3PbBr_3$ layer, $PbBr_2$ film was spin-coated on the PEDOT:PSS layer and annealed in CH_3NH_3Br vapor at 150°C for 2 h to form a perovskite layer under ambient condition. The quality of the perovskite layer was characterized by atomic force microcopy (AFM), X-ray diffraction (XRD) and scanning electron microscope (SEM) (Fig. 2). Different thicknesses of inorganic films were achieved through adjusting spin-coating rate from 2000 to 6000 rpm. The reaction time for forming the perovskite film was optimized to be 2 h. Thus, a planar perovskite layer was formed with different thicknesses ranging from 20 to 150 nm. The XRD analysis (Fig. 2a) indicates that a shorter reaction time results in the incomplete of $PbBr_2$, while a longer one contributes to higher roughness. In order to mark the appropriate reaction time, four samples were prepared. XRD clearly indicates that a film without CH_3NH_3Br is composed of $PbBr_2$. With increasing the reaction time, both $PbBr_2$ and $CH_3NH_3PbBr_3$ phases are confirmed. An obviously rising in $CH_3NH_3PbBr_3$ phase and decreasing in $PbBr_2$ phase are observed. A tiny peak in 18.6° corresponding to the trace $PbBr_2$ shows that the reaction time of 2 h is enough to change $PbBr_2$ to $CH_3NH_3PbBr_3$. Sharp diffraction peaks at 14.97° for (100) plane, 30.20° for (200), 45.93° for (300) exhibit well crystallization even under ambient condition according to the previous work [27]. Fig. 2b shows a low roughness and continuous layer with 2 h reaction time. Cross-sectional SEM in Fig. 2c demonstrates a planer morphology with three layers of ITO, PSS:PEDOT and $CH_3NH_3PbBr_3$. Longer time (4 h)

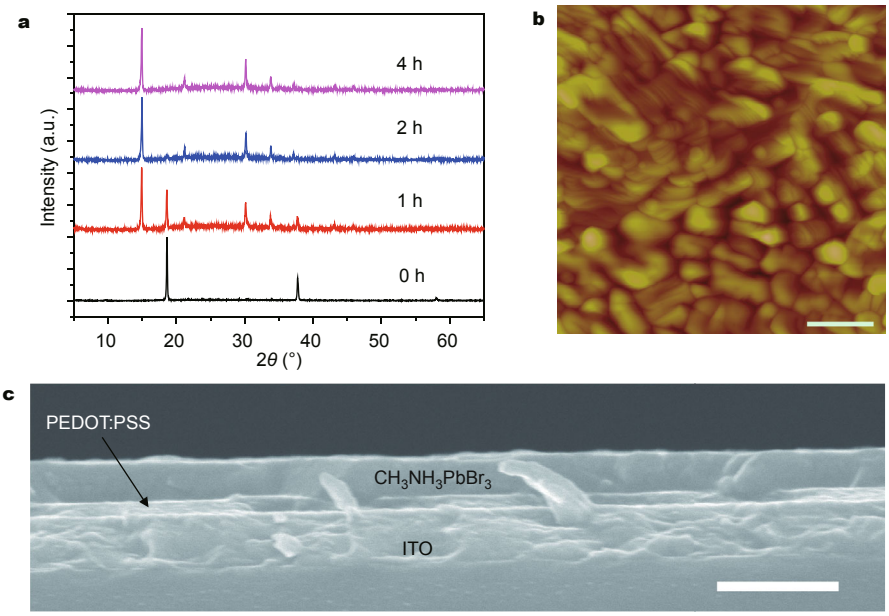

Figure 2 (a) Normalized XRD patterns for $PbBr_2$ film with CH_3NH_3Br vapor treated time from 0 to 4 h. (b) AFM image and (c) cross-sectional SEM image of the formed $CH_3NH_3PbBr_3$ layer after 2 h treatment of CH_3NH_3Br vapor. The scale bar is 1 μm for (b) and 200 nm for (c).

results in totally transforming to perovskite, but leads to a higher roughness, which should be avoided for a better device performance. The well crystallized film under atmosphere shows that $CH_3NH_3PbBr_3$ is not much affected by oxygen and moisture, which confirms that $CH_3NH_3PbBr_3$ is more stable than $CH_3NH_3PbI_3$ which decomposes at over 55% relative humidity [28].

The emission spectrum of $CH_3NH_3PbBr_3$ film is shown in Fig. 3. It can be seen that the electroluminescence spectrum reveals a strong peak at 536 nm, which is slightly blue-shifted compared with its photoluminescence spectrum with peak at 544 nm. It should be noted that the full width at half maximum of electroluminescence spectrum is narrowed to 20 nm, which indicates the high color purity. The structure of $CH_3NH_3PbBr_3$ is composed of two dimensional (2D) inorganic ($PbBr_2$) layer sandwiched between 2D organic (CH_3NH_3Br) layers. The significant dielectric constant difference between organic and inorganic layers contributes to the high color purity owing to the excitons confined in the inorganic layer [29,30]. The inset image shows an optical graph of the brightly green diode with 2 mm × 2 mm light emitting area.

Fig. 4 shows the device characteristics of the green perovskite LED. A typical diode *I-V* curve is demonstrated in Fig. 4a, which indicates a rapid increasing rate of current density. An obvious turn-on voltage of light-emission is observed at 3.5 V (Fig. 4b), which is a little higher than that of 3.3 V for a thinner emitter layer [23] owing to the increased

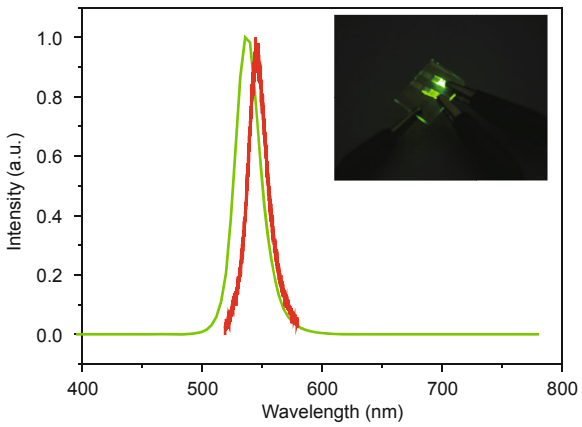

Figure 3 Normalized emission spectra of the $CH_3NH_3PbBr_3$ layer. Photoluminescence (red) at 544 nm and electroluminescence (green) at 536 nm. The inset image: green electroluminescence of the $CH_3NH_3PbBr_3$ LED.

thickness of the emitting layer. Thanks to the high-quality emitting layer, the luminance rises sharply to ~1000 cd m^{-2} at a current density of ~800 mA cm^{-2}. And the device exhibits a power efficiency of 0.1 lm W^{-1} with an EQE of 0.1% (Fig. 4c). Fig. 4d exhibits the relationship between the emitter thickness and the luminance properties. An obvious luminance rising is observed by increasing perovskite layer from 20 to 80 nm. And the device with 80 nm perovskite reveals the highest luminance upto 1500 cd cm^{-2}. Whereas, any further increase in perovskite thickness results in

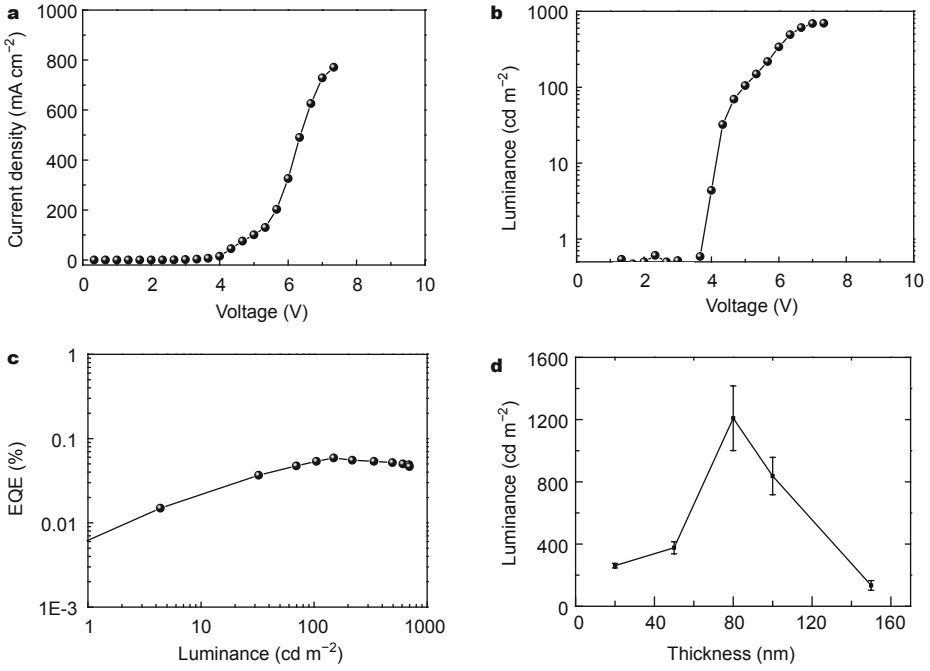

Figure 4 Device characteristics of the green perovskite LED tested in ambition condition. (a) Current density *vs*. voltage. (b) Luminance *vs*. voltage, the green diode turns on at 3.5 V. (c) EQE *vs*. luminance characteristics. (d) Luminance *vs*. the thickness of $CH_3NH_3PbBr_3$ layer.

the luminance decreasing owing to the higher roughness. Thus, the optimized emitter layer should be 80 nm in the perovskite LEDs. Moreover, these perovskite-LED devices exhibit good reproducibility, as illustrated by Fig. 4d based on measurement of 50 devices. The electroluminescence efficiency with a rising current density, corresponding to the previous work [23], demonstrates a need for high charge density for efficient recombination. Even though a higher luminance can be given with successive rising charge density, the electroluminescence efficiency decreases at high current density. In addition, a marked luminance decrease with a much higher current density was found due to the high temperature from the self-heat. Thus, it should be mentioned that an exceed voltage leads to a device broken, and thus an exceed current density should be avoided for a longtime electroluminescence and a higher efficiency.

In this work, a significant increase in electroluminescence is observed for perovskite-based LEDs with both increasing voltage and current density. Higher carrier recombination contributes to the increased electroluminescence luminance because of the high-quality emitter, whereas the EQE does not go up with the increased luminance. Large charge barriers and carrier quenching should take responsibility for the low EQE [31]. As shown in Fig. 1c, barrier potential for hole injecting from PEDOT:PSS to $CH_3NH_3PbBr_3$ is large because of the much deeper energy level of $CH_3NH_3PbBr_3$ than that of PEDOT:PSS. And the electron barrier is obvious attributed to the energy level mismatch of $CH_3NH_3PbBr_3$ and TmPyPB. Moreover, the interface roughness also lowers the EQE. For further study, appropriate hole transport and electron transport materials are essential for the higher efficiency.

In summary, high performance LED based on organic-inorganic halide perovskite ($CH_3NH_3PbBr_3$) was fabricated via a vapor assisted method under atmosphere. The devices exhibit high purity green electroluminescence characteristics at room temperature with a luminance at 1000 cd m^{-2} owing to the high quality emitting layer with full-coverage, well-crystallized and optimized thickness. It should be noted that a higher quality emitter for high current density is needed for a brighter emitting, and large carrier barriers create blocks for high efficiency. Meanwhile, the exceed current density can break the device quickly. It can be concluded that the organic-inorganic halide perovskites have great potential in optoelectronics or lighting fields and further researches on low toxicity, long-term stability and high luminance are expected.

Received 16 January 2015; accepted 13 February 2015; published online 16 March 2015

1 Burschka J, Pellet N, Moon SJ, *et al*. Sequential deposition as a route to high-performance perovskite-sensitized solar cells. Nature, 2013, 499: 316–319
2 Crossland EJ, Noel N, Sivaram V, *et al*. Mesoporous TiO_2 single crystals delivering enhanced mobility and optoelectronic device performance. Nature, 2013, 495: 215–219
3 Liu M, Johnston MB, Snaith HJ. Efficient planar heterojunction perovskite solar cells by vapour deposition. Nature, 2013, 501: 395–398
4 Jeon NJ, Noh JH, Yang WS, *et al*. Compositional engineering of perovskite materials for high-performance solar cells. Nature, 2015, 517: 476–480
5 Heo JH, Im SH, Noh JH, *et al*. Efficient inorganic-organic hybrid heterojunction solar cells containing perovskite compound and polymeric hole conductors. Nat Photonics, 2013, 7: 486–491
6 Mei A, Li X, Liu L, *et al*. A hole-conductor-free, fully printable mesoscopic perovskite solar cell with high stability. Science, 2014, 345: 295–298
7 Conings B, Baeten L, De Dobbelaere C, *et al*. Perovskite-based hybrid solar cells exceeding 10% efficiency with high reproducibility using a thin film sandwich approach. Adv Mater, 2013, 26: 2041–2046
8 Kazim S, Nazeeruddin MK, Gratzel M, *et al*. Perovskite as light harvester: a game changer in photovoltaics. Angew Chem Int Ed, 2014, 53: 2812–2824
9 Park NG. Organometal perovskite light absorbers toward a 20% efficiency low-cost solid-state mesoscopic solar cell. J Phys Chem Lett, 2013, 4: 2423–2429
10 Docampo P, Guldin S, Leijtens T, *et al*. Lessons learned: from dye-sensitized solar cells to all-solid-state hybrid devices. Adv Mater, 2014, 26: 4013–4030
11 Xing GC, Sun SY, Lim SS, *et al*. Long-range balanced electron-and hole-transport lengths in organic-inorganic $CH_3NH_3PbI_3$. Science, 2013, 342: 344–347
12 Stranks SD, Grancini G, Menelaou C, *et al*. Electron-hole diffusion lengths exceeding 1 micrometer in an organometal trihalide perovskite absorber. Science, 2013, 342: 341–344
13 Edri E, Kirmayer S, Henning A, *et al*. Why lead methylammonium triiodide perovskite-based solar cells require a mesoporous electron transporting scaffold (but not necessarily a hole conductor). Nano Lett, 2014, 14: 1000–1004
14 Zhao Y, Nardes AM, Zhu K. Solid-state mesostructured perovskite $CH_3NH_3PbI_3$ solar cells: charge transport, recombination, and diffusion length. J Phys Chem Lett, 2014, 5: 490–494
15 Ponseca CS, Savenije TJ, Abdellah M, *et al*. Organometal halide perovskite solar cell materials rationalized: ultrafast charge generation, high and microsecond-long balanced mobilities, and slow recombination. J Am Chem Soc, 2014, 136: 5189–5192
16 Stoumpos CC, Malliakas CD, Kanatzidis MG, *et al*. Semiconducting tin and lead iodide perovskites with organic cations: phase transitions, high mobilities, and near-infrared photoluminescent properties. Inorg Chem, 2013, 52: 9019–9038
17 Wehrenfennig C, Eperon GE, Johnston MB, *et al*. High charge carrier mobilities and lifetimes in organolead trihalide Perovskites. Adv Mater, 2014, 26: 1584–1589
18 Jung HS, Park NG. Perovskite solar cells: from materials to devices. Small, 2015, 11: 10–25
19 Xing G, Mathews N, Lim SS, *et al*. Low-temperature solution-processed wavelength-tunable perovskites for lasing. Nat Mater, 2014, 13: 476–480
20 Zhang Q, Ha ST, Liu X, *et al*. Room-temperature near-infrared high-Q perovskite whispering-gallery planar nanolasers. Nano Lett, 2014, 10: 5995–6001
21 Wehrenfennig C, Liu M, Snaith HJ, *et al*. Homogeneous emission line broadening in the organo lead halide perovskite $CH_3NH_3PbI_{3-x}Cl_x$. J Phys Chem Lett, 2014, 5: 1300–1306
22 Ha ST, Liu X, Zhang Q, *et al*. Synthesis of organic-inorganic lead halide perovskite nanoplatelets: towards high-performance per-

ovskite solar cells and optoelectronic devices. Adv Opt Mater, 2014, 2: 838–844
23 Tan ZK, Moghaddam RS, Lai ML, *et al*. Bright light-emitting diodes based on organometal halide perovskite. Nat Nanotechnol, 2014, 9: 687–692
24 Kim YH, Cho H, Heo JH, *et al*. Multicolored organic/inorganic hybrid perovskite light-emitting diodes. Adv Mater, doi: 10.1002/adma.201403751
25 Jeon NJ, Noh JH, Kim YC, *et al*. Solvent engineering for high-performance inorganic-organic hybrid perovskite solar cells. Nat Mater, 2014, 13: 897–903
26 Chen Q, Zhou H, Hong Z, *et al*. Planar heterojunction perovskite solar cells via vapor assisted solution process. J Am Chem Soc, 2014, 136: 622–625
27 Edri E, Kirmayer S, Kulbak M, *et al*. Chloride inclusion and hole transport material doping to improve methyl ammonium lead bromide perovskite-based high open-circuit voltage solar cells. J Phys Chem Lett, 2014, 5: 429–433
28 Noh JH, Im SH, Heo JH, *et al*. Chemical management for colorful, efficient, and stable inorganic-organic hybrid nanostructured solar cells. Nano Lett, 2013, 13: 1764–1769
29 Toshiaki H, Masanao E, Tetsuo T, *et al*. Highly efficient electroluminescence from a heterostructure device combined with emissive layered-perovskite and an electron-transporting organic compound. Chem Phys Lett, 1996, 254: 103–108
30 Era M, Morimoto S, Tsutsui T, Saito S. Organic-inorganic heterostructure electroluminescent device using a layered perovskite semiconductor $(C_6H_5C_2H_4NH_3)_2PbI_4$. Appl Phys Lett, 1994, 65: 676–678
31 Wei Z, Yan K, Chen H, *et al*. Cost-efficient clamping solar cells using candle soot for hole extraction from ambipolar perovskites. Energ Environ Sci, 2014, 7: 3326–3333

Acknowledgments The authors thank Ping He and Longfeng Jiang for help in the data analysis. This research was supported by the National Natural Science Foundation of China (51222306, 91222203, 91233205 and 91433115), the China-Denmark Co-project (60911130231), TRR61 (NSFC-DFG Transregio Project), the Ministry of Science and Technology of China (2011CB808405, 2011CB932304, 2013CB933403 and 2013CB933504), and the Strategic Priority Research Program of the Chinese Academy of Sciences (XDB12030300).

Author contributions Hu W and Dong H designed the experiments, conceived the post-fabrication tuning of the random modes; Qin X performed the experiments and wrote the paper with support by Hu W. All authors contributed to the general discussion.

Conflicts of interest The authors declare that they have no conflict of interest.

Xiang Qin received his BSc degree in chemistry from Peking University in 2012. He is currently studying for a PhD degree at the University of Chinese Academy of Sciences and his research interest focuses on organic field-effect transistors.

Huanli Dong was born in 1980. She is an associate professor of the Institute of Chemistry, Chinese Academy of Sciences (ICCAS). She received her MSc degree (2006) from Fujian Institute of Research on the Structure of Material, CAS, and PhD degree (2009) from the ICCAS. Her research focuses on molecular materials, crystals and devices. She has published more than 80 peer-reviewed papers with citation ~1800 times.

Wenping Hu received his PhD degree from the ICCAS, in 1999. Then he joined Osaka University and Stuttgart University as a research fellow of Japan Society for the Promotion of Sciences and Alexander von Humboldt, respectively. In 2003 he worked at Nippon Telephone and Telegraph (NTT), and then returned to the ICCAS, and became a full professor in 2003. His research focuses on organic/molecular electronics, and he has published more than 300 peer-reviewed papers with citation ~9000 times (h-index = 51).

中文摘要 有机金属卤化钙钛矿($CH_3NH_3PbX_3$)作为一种新型的半导体材料在光伏领域引起了广泛的关注. 同时, 有机金属卤化钙钛矿所拥有的光致发光以及较高荧光量子产率为其电致发光提供了可能. 因而, 研究有机金属卤化钙钛矿的电致发光行为对于进一步拓展其在光电领域的应用具有重要意义. 溴化钙钛矿($CH_3NH_3PbBr_3$)具备良好的光致发光性能, 具有较高的荧光量子产率, 同时在空气中具有较好的稳定性. 本文挑选$CH_3NH_3PbBr_3$作为发光层, 借用气体辅助法得到了高质量的$CH_3NH_3PbBr_3$薄膜, 并成功构建了发光二极管. 基于$CH_3NH_3PbBr_3$的发光二极管电致发光为536 nm的绿光, 发光亮度达到1000 cd m^{-2}, 外量子效率为0.1%. 该研究对于探索有机金属卤化钙钛矿的电致发光行为大有裨益, 同时也拓宽了有机金属卤化钙钛矿在光电领域的应用潜能.